Available online at www.sciencedirect.com
SCIENCE DIRECT®
Coordination Chemistry Reviews 249 (2005) 1410–1422
COORDINATION CHEMISTRY REVIEWS
www.elsevier.com/locate/ccr

Review

# Photoinduced electron transfer in supramolecular systems of fullerenes functionalized with ligands capable of binding to zinc porphyrins and zinc phthalocyanines☆

Francis D'Souza[a,*], Osamu Ito[b]

[a] *Department of Chemistry, Wichita State University, 1845 Fairmount, Wichita, KS 67260-0051, USA*
[b] *Institute of Multidisciplinary Research for Advanced Materials, Tohoku University, Katahira, Aoba-ku, Sendai 980-8577, Japan*

Received 1 August 2004; accepted 6 January 2005
Available online 6 February 2005

## Contents



## Abstract

This review describes light induced energy or electron transfer reactions in self-assembled supramolecular zinc porphyrin/zinc phthalocyanine and fullerene bearing donor–acceptor systems. The self-assembled supramolecular dyads and triads are formed by using one or two types of the binding mechanisms including metal–ligand axial coordination. The photochemical properties of the metal porphyrin/phthalocyanine and fullerene moieties are shown to be tuned in a controlled manner upon coordination of metal center. The nature of the linker between the donor and acceptor entities influences the overall self-assembly process followed by the photochemical reactivity. In these self-assembled supramolecular systems, the photoinduced charge separation occurs mainly from the excited singlet state of the donor; and the back electron transfer rates generally occurs giving reversible systems. In some of the reported donor–acceptor conjugates, the predicted acceleration of the charge separation process and deceleration of the charge recombination process have been clearly observed, mainly due to the small reorganization energies of fullerenes in electron transfer reactions. Elegantly designed supramolecular triads to achieve sequential electron transfer to obtain the charge-separated states, and sequential energy transfer followed by electron transfer to mimic the photosynthetic 'antenna-reaction center' have also been developed and studied. The relations between structures and photochemical reactivities of these novel supramolecular systems are discussed in relation to the efficiency of forward electron transfer and slowing down the charge recombination process.


*Keywords:* Porphyrins; Phthalocyanines; Fullerenes; Photoinduced electron transfer; Self-assembly; Supramolecules

☆ Published as part of the 15th International Symposium on the Photochemistry and Photophysics of Coordination Compounds, Hong Kong, 4–9 July.

* Corresponding author. Tel.: +1 316 978 7380; fax: +1 316 978 3431.
*E-mail addresses:* francis.dsouza@wichita.edu (F. D'Souza), ito@tagen.tohoku.ac.jp (O. Ito).

0010-8545/$ – see front matter © 2005 Elsevier B.V. All rights reserved.
doi:10.1016/j.ccr.2005.01.002

## 1. Introduction

The X-ray structures of the bacterial photosynthetic reaction centers have revealed that the electron donor and acceptor entities are arranged via non-covalent incorporation into a well-defined protein matrix [1–3]. The light induced electron transfer and energy transfer events occur between these well organized pigments. The charge separation occurs with remarkable high efficiency with spatially and electronically well-isolated radical ion pair while eliminating the energy wasting back electron transfer. The small overall reorganization energy ($\lambda \sim 0.2$ eV) exhibited by the photosynthetic reaction center and the well-balanced electronic coupling between the electron donor and acceptor entities have been attributed to the high efficiency of charge separation.

Development of relatively simple, donor–acceptor model systems to mimic the events of the photosynthetic reaction center has been one of the important goals of chemistry during the past two decades [4–36]. Two main applications, in general, have been sought out from these model compounds. First, conversion of solar energy into chemical energy [4–36], and second, utilizing these compounds in the development of optoelectronic devices [37,38]. In order to increase the rate of forward electron transfer and to slow down the charge recombination, improved model compounds with well-adjusted energies of the donor and acceptor molecules, and finely tuned electronic coupling between the donor and acceptor entities have been elegantly designed and studied. In some cases, long-lived charge-separated states have been achieved by incorporating a secondary electron donor or acceptor entities into multicomponent arrays such as triads, tetrads, pentads, etc.

Fullerenes have been widely utilized as three dimensional electron acceptors [39–41]. Fullerenes ($C_{60}$/$C_{70}$) exhibit a number of characteristic electronic and photophysical properties, which make them promising candidates for building donor–acceptor model compounds for the study of electron transfer processes. Among these, the most noteworthy property is the small reorganization energy associated in light induced electron transfer reactions [42–44]. This property has been regarded as one of the important requisite for the directional control and efficiency of electron transfer reactions, as revealed by the electron transfer reactions of photosynthetic reaction center. Generally, the photoinduced charge transfer occurs in the 'normal region' of the Marcus curve while the charge recombination occurs in the 'inverted region' of the Marcus curve for electron transfer involving porphyrin–fullerene dyads. The small reorganization energy is due to the fullerene's unique structure and symmetry, which is ultimately responsible for its high degree of delocalization and structural rigidity [39]. In addition, fullerenes have the first reduction potentials comparable to that of benzoquinone [45–47], and can reversibly accept up to six electrons [48–51]. A more practical aspect of $C_{60}$ and $C_{70}$ concerns the optical absorption spectra of their π-radical anions, such as $C_{60}^{\bullet -}$ and $C_{70}^{\bullet -}$, which show narrow bands in the near-IR region, around 1080 and 1380 nm, respectively, serving as diagnostic probes for their identification [41,52–56]. These isolated absorptions allow an accurate analysis of inter- and intramolecular electron transfer dynamics of $C_{60}$ and $C_{70}$. For example, nanosecond transient absorption spectra for intermolecular electron transfer system of $C_{60}$ and zinc phthalocyanine (ZnPc) in benzonitrile (PhCN) are shown in Fig. 1, in which the excited triplet state of ZnPc ($^3$ZnPc$^*$) appeared at 600 and 750 nm immediately after the selective excitation of ZnPc in the presence of $C_{60}$. With the concomitant decay of $^3$ZnPc$^*$, the radical cation of ZnPc (ZnPc$^{\bullet +}$) and radical anion of $C_{60}$ ($C_{60}^{\bullet -}$) appeared at 970 and 1080 nm, respectively, suggesting intermolecular electron transfer from $^3$ZnPc$^*$ to $C_{60}$ [57]. By the selective excitation of $C_{60}$ in the presence of ZnPc, intermolecular electron transfer from ZnPc to $^3C_{60}{}^*$ was also confirmed by the decay of $^3C_{60}{}^*$ at 740 nm and rises of ZnPc$^{\bullet +}$ and $C_{60}^{\bullet -}$ [58]. Since the overlaps of these transient absorption bands are minimum, the rate constants and quantum yields were accurately evaluated.

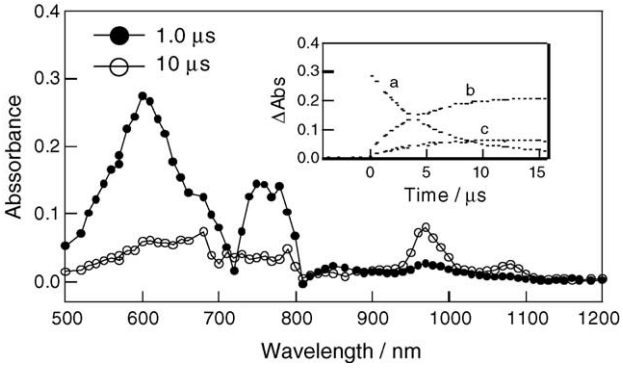


Fig. 1. Nanosecond transient absorption spectra obtained by 650 nm laser light excitation of ZnNc (0.1 mM) in the presence of pristine $C_{60}$ (0.1 mM) in PhCN. Inset: time-profiles of (a) 600 nm; (b) 970 nm (3×); and (c) 1080 nm (3×).

Owing to their importance and above listed unique properties, several donor–acceptor systems featuring fullerenes as electron acceptors have been elegantly designed, synthesized and studied [42–50]. A vast majority of the systems utilized porphyrins, phthalocyanines, or metal trispyridyl complexes as primary electron donors covalently linked to the fullerene acceptors. Additionally, a number of model compounds involving covalently linked triads, tetrads, etc., have been designed and the much desired long-lived charge-separated states have been achieved [59–65]. Using the fullerene–porphyrin modified electrodes, photoelectrochemical cells have also been constructed for direct conversion of light energy in electrical energy [66]. In several instances, high efficiency of light-energy conversion has been achieved. More recently, an increasing number of non-covalently linked donor–acceptor supramolecular assemblies have also been studied [36]. Due to the more biomimetic nature of the biological electron transfer systems, non-covalently linked self-assembled donor–acceptor systems are more appealing as model compounds. Also, the

self-assembled supramolecules offer significant advantages over the covalently linked ones for construction of complex multi-component structures. It may be mentioned here that fullerene also forms co-crystallites with metalloporphyrins [67], similar to that observed in $C_{60}$(ferrocene)$_2$ [68]. Here, the interaction between the fullerene and the metal complexes is mainly van der Waals in origin.

The purpose of this review is to summarize the results of self-assembled supramolecular systems featuring fullerenes as acceptors and porphyrin/phthalocyanine as donors. Porphyrins and phthalocyanines as donors are attractive not only due to their resemblance to naturally occurring tetrapyrroles, but also due to their well-characterized photochemical/photophysical properties such as their relatively high absorbance in the visible region and their high electron–donor abilities, so that they are suitable for efficient electron transfer in the ground and excited states [69–73]. Importantly, the porphyrin macrocycle is capable of binding a variety of transition metals within its central cavity, thus leaving the positions axial to the plane of the porphyrin ring available for binding with a variety of ligands [36].

In the studied self-assembled supramolecular porphyrin/phthalocyanine-fullerene systems, the donor and acceptor entities are functionalized in such a way that the two entities are able to reversibly bind in solution. The modes of binding often employed axial ligation via nitrogen-based ligands to the metal center of the metallo-porphyrins/ metallophthalocyanines. Several factors govern the electron transfer rates in the self-assembled donor–acceptor systems; some of them are regarded to be advantages over the covalently linked analogs. These advantages include (i) control over the relative orientation of the donor and acceptor that has been achieved in some cases, which is quite important, since electron transfer rates are dependent upon orbital overlap and distance between the donor and acceptor moieties. (ii) The electron transfer is governed by binding strength, and concentration of the donor and acceptor entities. (iii) By properly adjusting the concentrations of the donor and acceptor entities to achieve sufficient amount (>99%) of complexed species in solution, most of the electron transfer can be made to occur from the short-lived singlet excited state of the donor or acceptor entity. (iv) Since the binding of the donor–acceptor complex is reversible in nature, after the occurrence of electron transfer, the individual charge-separated species ($D^{\bullet+}$ and $A^{\bullet-}$) can diffuse away from each other, creating a long-lived solvent separated ion pairs in a sufficiently polar medium; thus, increasing the lifetime of the charge-separated state.

## 2. Supramolecular fullerene–zinc porphyrin/zinc phthalocyanine conjugates

### *2.1. Fullerene–zinc porphyrin/zinc phthalocyanine systems coordinated via axial ligation*

As pointed out earlier, the porphyrin macrocycle is capable of binding a variety of transition metals within its central cavity, thus leaving the positions axial to the plane of the porphyrin ring available for binding with a variety of ligands [36,74–85]. In 1999, three different research groups studied systems composed of $C_{60}$ functionalized with a coordinating ligand capable of axially ligating to the metalloporphyrin metal center (ZnTPP and RuTPP) [82–84].

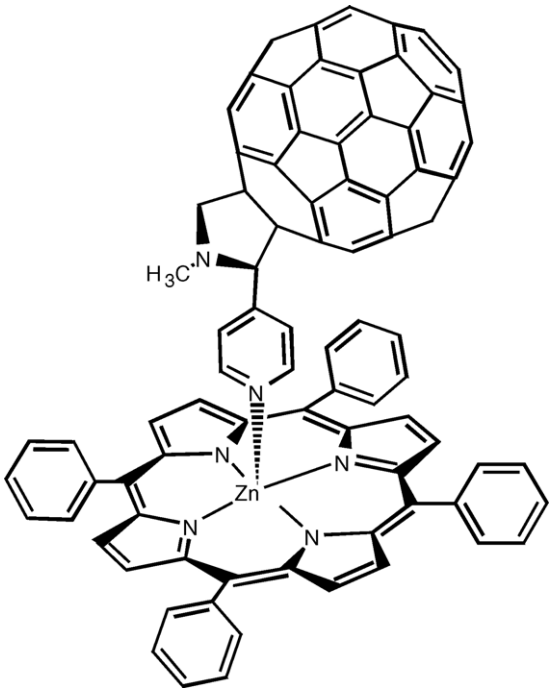


Fig. 2. Structure of zinc tetraphenylporphyrin←(4-pyridyl)fulleropyrrolidine conjugate.

Our research groups performed a systematic study on donor–acceptor systems composed of $C_{60}$ bearing nitrogen-based ligands (*o*-pyridyl, *m*-pyridyl, *p*-pyridyl (Fig. 2), *N*-phenyl imidazole) axially ligated to ZnTPP [79]. UV–vis spectral data were used to determine the binding constants (*K*) for each $C_{60}$ derivative with ZnTPP. The trend observed for the *K*-values was: *o*-pyridyl $\ll$ *m*-pyridyl $\approx$ *p*-pyridyl $\ll$ *N*-phenyl imidazole. Thermodynamic parameters for these systems suggested that both enthalpy and entropy changes contribute to the overall free-energy changes for the self-assembly of the systems.

X-ray structural and ab initio computational studies on of the supramolecules involving *p*-pyridyl derivatized fulleropyrrolidine and ZnTPP were also performed [85]. In the studied solid state structure (Fig. 3), the zinc-to-axially coordinated pyridyl nitrogen distance was found to be 2.158 Å which is compatible with a 2.075 Å average distance of the porphyrin ring Zn–N bonds. Importantly, the center-to-center distance between the porphyrin zinc ion and fullerene was ca. 9.53 Å. Additional intermolecular interactions between the zinc porphyrin and the $C_{60}$ unit that is not directly coordinated to the zinc were also observed in the crystal packing.

Our research groups recently prepared and studied a supramolecular dyad system composed of an imidazole-

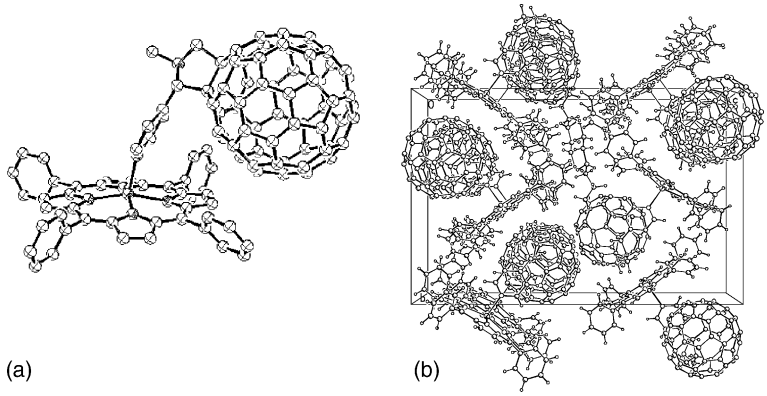


Fig. 3. (a) Projection diagram of the axially coordinated ZnTPP and *N*-methyl-2-(pyrid-4′-yl)-3,4-fulleropyrrolidine complex with 50% thermal ellipsoids. (b) Packing diagram (from Ref. [85]).

appended $C_{60}$ ($C_{60}$∼Im), which axially coordinates via the imidazole nitrogen to the central metal of zinc naphthalocyanine (ZnNc) [57]. UV–vis spectral data were used to confirm the formation of the self-assembled dyad system (Fig. 4). Upon addition of $C_{60}$∼Im to a solution containing ZnNc (toluene), the absorption band at 767 nm exhibited diminished intensity, and isosbestic points appeared at 675, 717, 752, and 791 nm. The *K*-value for the dyad in toluene solution was determined to be $6.2 \times 10^4\ M^{-1}$ by the Scatchard method. This value is an order of magnitude larger than that of the counterpart ZnTPP dyad system.

Molecular orbital calculations by ab initio B3LYP/3-21G(*) method gave an optimized structure of ($C_{60}$∼Im→ZnNc; the symbol '→' refers to a coordination bond) as shown in Fig. 5, in which the HOMO and LUMO are illustrated. The electron densities of the HOMO localized in the ZnPc moiety, while the electron densities of the LUMO localized in the $C_{60}$ moiety in $C_{60}$∼Im, suggesting that the charge-separated state of the supramolecular is $C_{60}^{\bullet -}$∼Im→$ZnNc^{\bullet +}$.

Steady-state fluorescence experiments were performed on the self-assembled dyad system. Upon addition of $C_{60}$∼Im to a solution containing ZnNc (toluene or *o*-dichlorobenzene (*o*-DCB)), the emission bands at 781 and 812 (sh) nm were gradually quenched to about 30% of the original intensity. Also, the emission band at 781 nm experiences a 3-nm blue shift compared to the original uncoordinated ZnNc. Stern–Volmer plots were used to determine the quenching constant for the dyad system. This value was determined to be four orders of magnitude larger than what would be expected for a diffusion-controlled dynamic quenching process. This indicates that an intramolecular quenching process is the predominant quenching pathway for the dyad system.

Time-resolved fluorescence spectral studies were performed on the dyad system. The excited state of pure ZnNc had a lifetime of 2.42 ns. Upon addition of $C_{60}$∼Im to form $C_{60}$∼Im→ZnNc, the excited state decayed bi-exponentially, having both fast and slow components (Fig. 6). The fast component had a lifetime of around 71 ps, while the slow component had a lifetime of around 2.14 ns. The slow component lifetime was similar to that obtained for uncomplexed ZnNc. The short-lived nature of the excited state of ZnNc in $C_{60}$∼Im→ZnNc suggests quenching via electron transfer from $^1ZnNc^*$ to the $C_{60}$ moiety in $C_{60}$∼Im. The $k_{CS}$ value

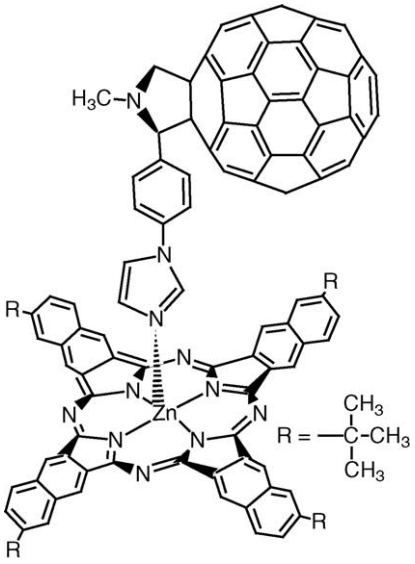


Fig. 4. Structure of $C_{60}$∼Im→ZnNc self-assembled via axial ligation conjugate.

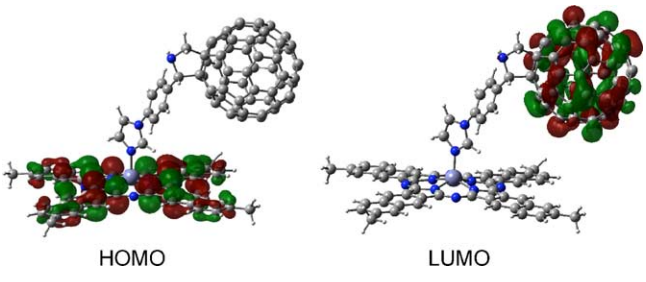


Fig. 5. Ab initio B3LYP/3-21G(*) calculated HOMO and LUMO orbitals of $C_{60}$∼Im→ZnNc dyad. *t*-Butyl groups of ZnNc are replaced by methyl groups and *N*-methyl group of $C_{60}$∼Im isreplaced by H atom.

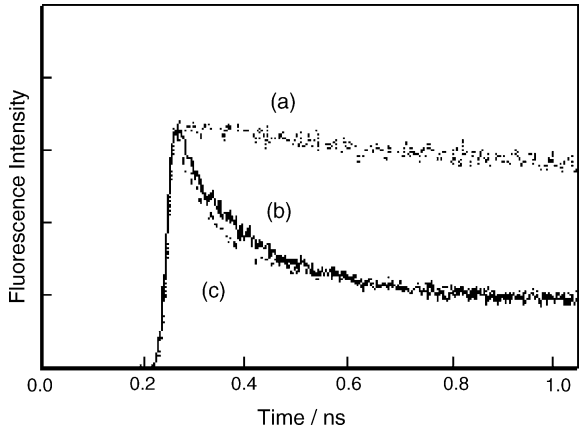


Fig. 6. Fluorescence decay time-profiles monitored at 700–750 nm: (a) ZnNc; (b) ZnNc + $C_{60}$Im (0.1 mM); and (c) ZnNc + $C_{60}$∼Im (0.2 mM) in toluene, $\lambda_{ex}$ = 410 nm.

was determined to be $1.4 \times 10^{10}\ s^{-1}$, with a $\Phi_{CS}$ value of 0.97 for the charge-separation process in toluene.

Picosecond transient absorption spectra were obtained in order to determine the nature of the excited state photochemical reactions in this time domain. Upon excitation of the dyad with 388-nm laser light, broad absorption bands appeared in 400–1100 nm immediately after the 150 fs laser pulse (spectrum at 10 ps in Fig. 7), which were attributed to the $S_1 \rightarrow S_n$ transitions of the ZnNc and $C_{60}$ moieties. Afterward new bands appeared at 710 and 985 nm as shown in the spectrum at 200 ps in Fig. 7. These bands were attributed to the formation of $ZnNc^{\bullet+}$. The band expected at 1000 nm representing $C_{60}{}^{\bullet-}$∼Im was not observed, probably due to masking by the intense band at 985 nm. The $k_{CS}$ value for the dyad was evaluated to be $1.4 \times 10^{10}\ s^{-1}$, which is in agreement with the value determined by fluorescence lifetime measurements, while the $k_{CR}$ value was evaluated to be $8.5 \times 10^{8}\ s^{-1}$.

Nanosecond transient absorption spectra were also obtained for the self-assembled dyad (Fig. 8). Upon excitation of $C_{60}$∼Im→ZnNc with 532-nm laser light, absorption bands were observed in the region of 960–1000 nm after 10 ns, corresponding to the formation of $C_{60}{}^{\bullet-}$∼Im→$ZnNc^{\bullet+}$. These absorption bands show quick decay behavior, indicating a rapid charge recombination process. Intense broad absorption bands observed between 600–700 and 830 nm after 100 ns correspond to $^3ZnNc^*$ and $^3C_{60}{}^*$∼Im, which may be produced by the intersystem crossing (ISC) process of uncomplexed constituents.

The transient absorption spectra in coordinating solvents such as PhCN were quite different. Upon excitation of the dyad with 650-nm laser light, the transient spectra similar to those in Fig. 1 were observed, exhibiting the band at 600 nm, which was attributed to appreciable population of $^3ZnNc^*$. With the decay of the absorption band of $^3ZnNc^*$, the rise of the absorption bands in the 960–1000 nm region was observed, which was attributed to the formation of the radical ions, $ZnNc^{\bullet+}$ and $C_{60}{}^{\bullet-}$∼Im. These data suggest that in a coordinating solvent the intermolecular electron transfer

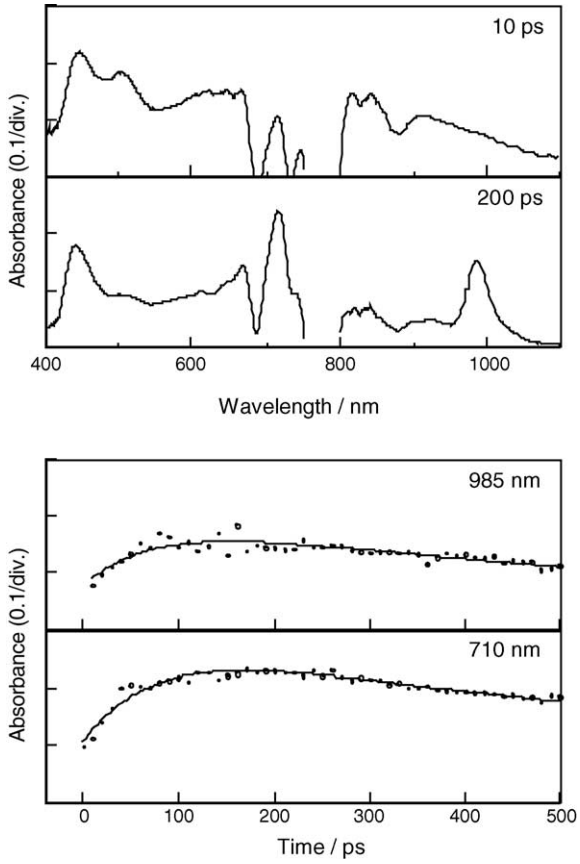


Fig. 7. Picosecond transient absorption spectra of ZnNc in the presence of $C_{60}$∼Im (0.1 mM) in *o*-DCB and time-profiles.

process takes place from $^3ZnNc^*$ to $C_{60}$∼Im. The bimolecular electron transfer rate constant ($k_{ET}$) was evaluated to be $1.3 \times 10^{8}\ M^{-1}\ s^{-1}$. The decays of $ZnNc^{\bullet+}$ and $C_{60}{}^{\bullet-}$∼Im obey second-order kinetics suggesting that both radical ions are separately solvated in PhCN. The back electron transfer rate constant ($k_{BET}$) was determined to be $3.6 \times 10^{9}\ M^{-1}\ s^{-1}$. The energy diagrams are shown in Fig. 9, in which the intrasupramolecular charge-separation takes place via $^1ZnNc^*$, since the $k_{CS}$ value is larger than the $k_{ISC}$ value. On the other hand, intermolecular electron transfer takes place in

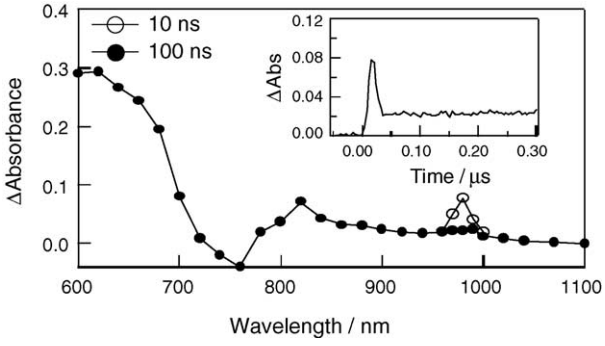


Fig. 8. Nanosecond transient spectra (532 nm laser light excitation) of $C_{60}$∼Im→ZnNc (1:1 equiv., 0.1 mM) in toluene. Inset: time-profile at 1000 nm.

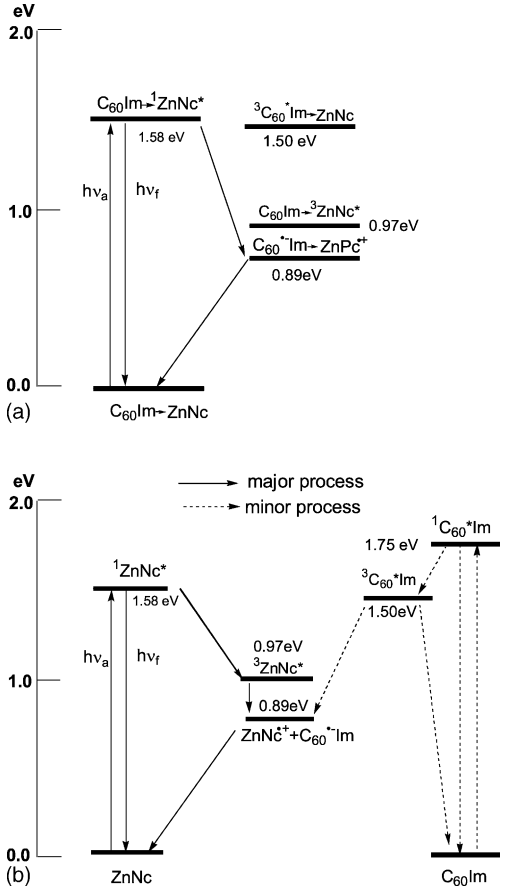


Fig. 9. Energy level diagrams showing different photochemical events of (a) intra-supramolecular dyad, $C_{60}$∼Im→ZnNc and (b) intermolecular excited state processes occurring between ZnNc and $C_{60}$∼Im. Energy level of $^3C_{60}^*$∼Im is lower limit.

the millisecond order as shown in Fig. 1, the value of $k_{ET}$ [$C_{60}$] is smaller than the $k_{ISC}$ value.

Recently, Wilson et al. [86] also developed and studied a dyad system composed of a pyridine-appended $C_{60}$ that axially ligates to the central metal of ZnTPP with a linear geometry. Armaloli et al. studied another dyad [83]. This dyad was composed of a pyridine-appended $C_{60}$ molecule ($C_{60}$∼Py) synthesized by Bingel addition to the fullerene, which can axially coordinate to ZnTPP via the central metal atom.

Our research groups recently prepared and studied a novel triad system composed of a zinc porphyrin appended with hydrogen-bonding groups such as either a carboxylic acid or an amide group (ZnP∼$CO_2$H or ZnP∼$NH_2$) and a $C_{60}$ molecule appended with a pyridine group and a *N*,*N*-dimethylaniline (DMA) group ($C_{60}$∼DMA(∼Py)) [87]. The triad $C_{60}$∼DMA(∼Py) is self-assembled via a "two-point" binding motif, where the pyridine group on the $C_{60}$ axially ligates to the central metal of the zinc porphyrin, while the nitrogen of the fulleropyrrolidine ring hydrogen bonds with the hydrogen-bonding group attached to ZnP, either ZnP∼$CO_2$H or ZnP∼$NH_2$.

UV–vis, $^1$H NMR, and ab initio B3LYP/3-21G(*) computational studies were used to verify the integrity of the self-assembled triads. Upon addition of $C_{60}$∼DMA to a solution containing either ZnP∼$CO_2$H or ZnP∼$NH_2$, a characteristic decrease and red shift of the Soret band were observed. Also, upon addition of either ZnP∼$CO_2$H or ZnP∼$NH_2$ to a solution of $C_{60}$∼DMA(∼Py), the pyridine and fullerpyrrolidine protons experienced an upfield shift caused by interaction with the ring current of the porphyrin ring, while the amide and carboxylic acid protons experienced a downfield shift due to hydrogen bonding interactions. These results clearly indicated the formation of the supramolecular triad system via the "two-point" binding motif. The *K*-values for the triads $C_{60}$∼DMA(∼Py)→ZnP∼$CO_2$H and $C_{60}$∼DMA(∼Py)→ZnP∼$NH_2$ were evaluated via Scatchard plots and were determined to be $10 \times 10^4$ and $3.1 \times 10^4$ $M^{-1}$, respectively.

Upon addition of $C_{60}$∼DMA(∼Py) to a solution containing either ZnP∼$CO_2$H or ZnP∼$NH_2$ in *o*-DCB, the fluorescence intensity of the ZnTPP moiety was efficiently quenched to about 30% of its original value. Also, a weak band at 710 nm, corresponding to the emission of $C_{60}$, was observed, suggesting energy transfer.

Upon complexation with $C_{60}$∼DMA(∼Py), fast fluorescence decay of $^1$ZnTPP$^*$ was found to be more efficient for the "two-point" bound systems as compared with the singly bound counterpart. These data indicate that the DMA moiety acts as a secondary electron donor and accelerates the charges separation process.

Nanosecond transient absorption spectra of $C_{60}$∼DMA(∼Py)→ZnP∼$NH_2$ exhibited band at 1000 nm corresponding to $C_{60}^{\bullet-}$∼DMA(∼Py), in addition to the bands at 700 and 870 nm for $^3C_{60}^*$∼DMA(∼Py) and $^3$ZnP$^*$∼$NH_2$, respectively. The $C_{60}^{\bullet-}$∼DMA(∼Py) band at 1000 nm was still observed in the transient absorption spectra after 0.25 μs, indicating that the DMA group aids in the stabilization of the charges separation state.

The relatively strong binding in the "two-point" bound triad system is thought to play a role in the increased stabilization of the charge-separated state. A comparison of the ratio $k_{CS}/k_{CR}$, which reflects the electron transfer efficiency, shows that as the *K*-values increase for the "two-point" bound system, so does $k_{CS}/k_{CR}$. This indicates that for the more strongly bound systems the efficiency of the ET process increases. Also, the DMA group is thought to play a role in slowing down charge recombination and thereby increasing the lifetime of the charges separation state for the triad system. Since the $E_{ox}$ value of the DMA group is relatively low, after initial charge separation generating ZnP$^{\bullet+}$∼$NH_2$ and $C_{60}^{\bullet-}$∼DMA(∼Py), the DMA group donates an electron to ZnP$^{\bullet+}$∼$NH_2$. Thus, a hole shift occurs from ZnP$^{\bullet+}$∼$NH_2$ to the DMA group, which is stable owing to the irreversible nature of the DMA oxidation. These processes are thought to be the mechanism of the slow charge recombination that is observed.

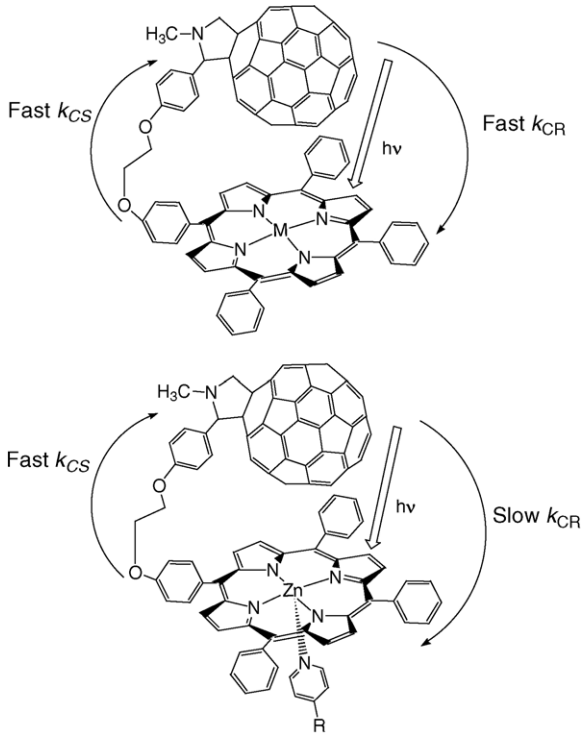


Fig. 10. Proposed mechanism of photochemical charge stabilization by coordination of pyridine to ZnP∼$C_{60}$ dyads.

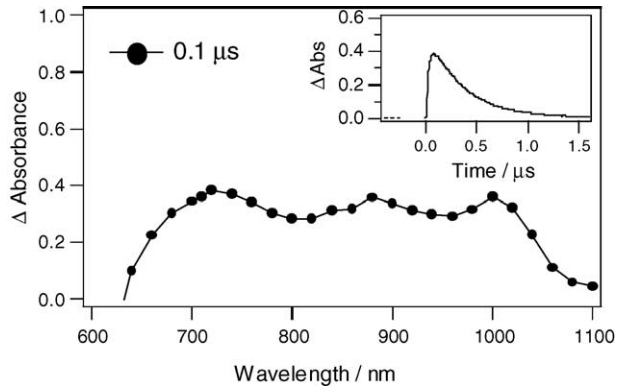


Fig. 11. Nanosecond transient absorption spectra obtained using 532 nm laser excitation of ZnP∼$C_{60}$ (0.1 mM) in Ar-saturated neat pyridine. Inset: Time-profile for 1000 nm band.

### 2.2. Pyridine addition effect on fullerene–zinc porphyrin dyads

In *o*-DCB, Zn∼$C_{60}$ dyads (Fig. 10) showed the relatively short lifetimes of the charge-separated state compared with long lifetime in benzonitrile [88]. On addition of small amount of pyridine to *o*-DCB solution, the lifetimes of the charge-separated states of Py→ZnP∼$C_{60}$ triads prolong as shown in Fig. 11. The pyridine addition effect on the lifetimes of the charge-separated state in *o*-DCB was as large as 50–100 times. For the reasons, steric factor and electronic factors can be considered. On coordination of pyridine to ZnP generation Py→ZnP∼$C_{60}$, the conformation of $C_{60}$ and ZnP in $C_{60}$∼ZnP may change. As for electronic factors, coordinated pyridine promotes the donor ability of ZnP and, furthermore, hole on ZnP in the charge-separated state delocalizes on to the coordinated pyridine moiety. Local polarity may be also change by the pyridine coordination.

### 2.3. Hole-shifting effect of ferrocene connected with zinc porphyrins

A new series of supramolecular triads were constructed by using covalently linked zinc porphyrin–ferrocene(s) dyads (ZnP∼Fc **1**–**3** in Fig. 12), self-assembled via axial coordination to either $C_{60}$∼Py or $C_{60}$∼Im [89]. In these supramolecular triads, the magnitude of the binding constants (*K*) from optical absorption studies, and the optimized geometry ob-

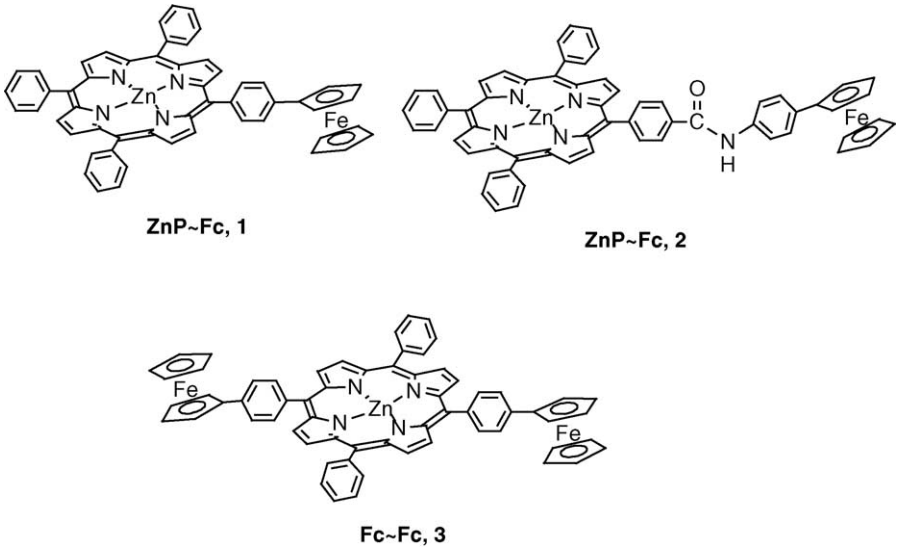


Fig. 12. Structure of the zinc porphyrin–ferrocene(s) dyads utilized for form supramolecular triads via axial coordination of functionalized fullerenes.

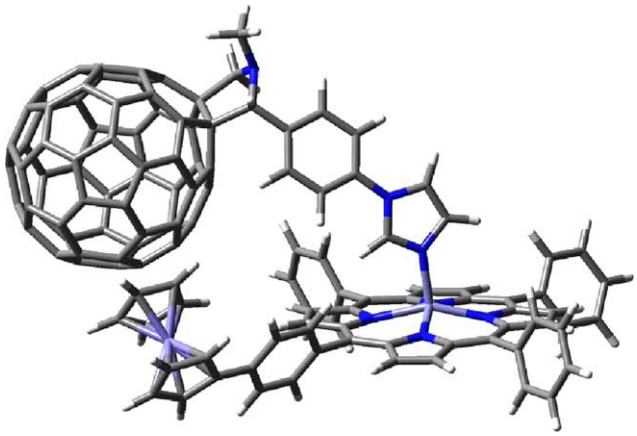

Fig. 13. Ab initio B3LYP/3-21G(*) optimized geometry of tsupramolecular triad formed by $C_{60}$∼Im and **1**.

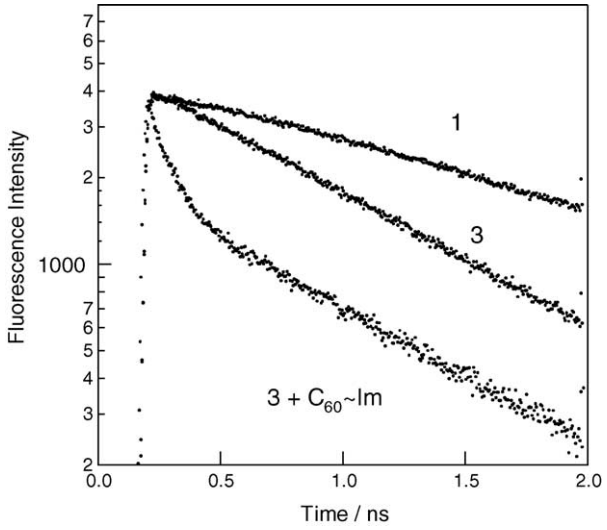


Fig. 14. Fluorescence decay profiles of **1** (0.05 mM), **2** (0.05 mM), and **3** (0.05 mM) + $C_{60}$∼Im (0.50 mM) in Ar-saturated *o*-DCB.

tained by ab initio B3LYP/3-21G(*) methods revealed the existence of intermolecular interactions between the ferrocene and fullerene entities, as shown for the $C_{60}$∼Im→ZnP∼Fc complex in Fig. 13. Photoinduced charge-separation and charge-recombination processes were examined in the dyads and triads by means of time-resolved fluorescence lifetime measurements (Fig. 14). In the case of the ZnP∼Fc dyads, upon photoexcitation, efficient ($\Phi_{CS} = 0.98$) to moderate ($\Phi_{CS} = 0.54$) amounts of electron transfer from the ferrocene to the singlet excited zinc porphyrin occurred depending upon the nature of the spacer (Table 1), resulting in the formations of $Fc^{+}$∼$ZnP^{\bullet -}$ radical ion-pairs, which are usually short-lived (≪10 ns). Upon forming the supramolecular triads by axial coordination $C_{60}$∼Im→ZnP∼Fc, the fluorescence lifetime became shorter, suggesting that the initial efficient charge-separation originated from the $^{1}ZnP^{*}$ moiety to the $C_{60}$ moiety takes place, generating $C_{60}^{\bullet -}$∼Im→$ZnP^{\bullet +}$∼Fc with high quantum efficiency. The nanosecond transient spectra (Fig. 15a) showed the appearance of the absorption bands at <500 and 1000 nm, which are attributed to the $ZnP^{\bullet +}$ and $C_{60}^{\bullet -}$ moieties, respectively. The calculated ratio of $k_{CS}/k_{CR}$ from the kinetic data was found to be ∼100 indicating moderate amount of charge stabilization in the studied supramolecular triads (Table 1). Although it was expected to shift of the hole from $ZnP^{\bullet +}$ to Fc, ultimately transforms into the final charge-separated states of $C_{60}^{\bullet -}$∼Im→ZnP ZnP∼$Fc^{+}$, the almost the same decay rates of $ZnP^{\bullet +}$ and $C_{60}^{\bullet -}$ in Fig. 15b and c indicate that such hole transfer is competitive with the charge recombination between $ZnP^{\bullet +}$ and $C_{60}^{\bullet -}$.

### *2.4. Energy transfer followed by electron transfer in a supramolecular triad composed of porphyrin, fullerene, and antenna molecules*

Recently, a working model of the photosynthetic antenna-reaction center complex, constructed via self-assembled supramolecular methodology, was reported [90]. For this, a supramolecular triad was assembled by axially coordinating $C_{60}$∼Im to the zinc center of a covalently linked

Table 1
Fluorescence lifetimes ($\tau_f$), charge-separation rate-constants ($k_{CS}$)[a], and charge separation quantum-yields ($\Phi_{CS}$) for zinc porphyrin–ferrocene(s) dyads and triads formed by axial coordination of fulleropyrrolidines in *o*-DCB [89]

| Compound[b] | $\tau_f$ (ps, fra %) | | $k_{CS}$ ($s^{-1}$) | $\Phi_{CS}$ | $k_{CS}$ ($s^{-1}$) | $\Phi_{CS}$ | $k_{CR}$ ($s^{-1}$) |
|---|---|---|---|---|---|---|---|
| | | | $^{1}ZnP^{*}$∼Fc | | $C_{60}$→$^{1}ZnP^{*}$ | | |
| ZnTPP | 1920 (100) | | | | | | |
| **1** | 40 (100) | | $2.5 \times 10^{10}$ | 0.98 | | | |
| **2** | 890 (100) | | $6.0 \times 10^{8}$ | 0.54 | | | |
| **3** | 35 (100) | | $2.8 \times 10^{10}$ | 0.98 | | | |
| $C_{60}$∼Py→**1**[c] | 40 (100) | | $2.5 \times 10^{10}$ | 0.98 | | | $2.6 \times 10^{8}$ |
| $C_{60}$∼Py→**2**[c] | 40 (100) | | $2.5 \times 10^{10}$ | 0.98 | | | $1.7 \times 10^{8}$ |
| $C_{60}$∼Py→**3**[c] | 80 (31) | 890 (69 %) | $6.0 \times 10^{8}$ | 0.54 | $1.2 \times 10^{10}$ | 0.96 | $1.3 \times 10^{8}$ |
| $C_{60}$∼Im→**1**[c] | 80 (68) | 890 (32 %) | $6.0 \times 10^{8}$ | 0.54 | $1.2 \times 10^{10}$ | 0.96 | $1.2 \times 10^{8}$ |
| $C_{60}$∼Im→**2**[c] | 35 (100) | | $2.8 \times 10^{10}$ | 0.98 | | | |
| $C_{60}$∼Im→**3**[c] | 35 (100) | | $2.8 \times 10^{10}$ | 0.98 | | | |

[a] $k_{CS}^{singlet} = (1/\tau_f)_{sample} - (1/\tau_f)_{ref}$, $^{*}\Phi_{CS}^{singlet} = [(1/\tau_f)_{sample} - (1/\tau_f)_{ref}]/(1/\tau_f)_{sample}$. For bi-exponential fitting, $\tau_f$ from the initial decay component was employed.
[b] For abbreviations, see Fig. 12.
[c] [Porphyrin] = 0.05 mM; [fullerene] = 0.50 mM.

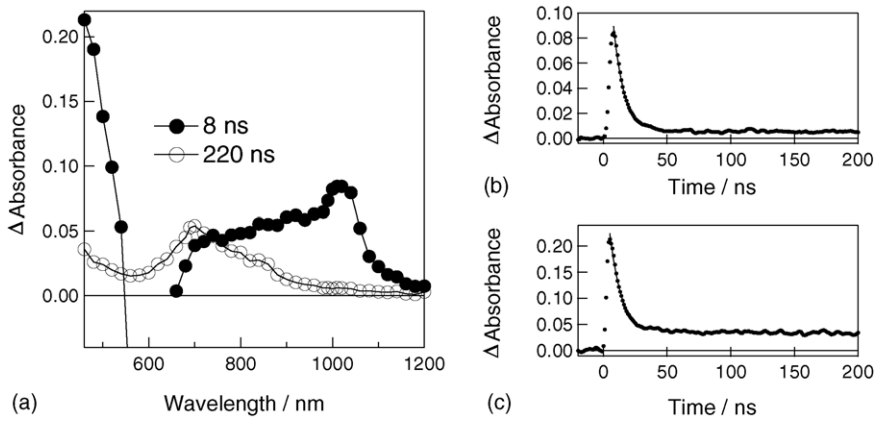


Fig. 15. (a) Nanosecond transient absorption spectra of $C_{60}$∼Im→3 (0.5: 0.1 mM) in *o*-DCB at 8 ns (●) and 220 ns (○) after 565 nm-laser irradiation. Absorption–time profiles monitored at (b) 1010 nm and (c) 460 nm.

zinc porphyrin–boron dipyrrin dyad (ZnP∼BDP) (Fig. 16). Selective excitation of the boron dipyrrin moiety in the boron dipyrrin–zinc porphyrin dyad resulted in efficient energy transfer ($k_{ENT}^{singlet} = 9.2 \times 10^9\ s^{-1}$; $\Phi_{ENT}^{singlet} = 0.83$) creating $^1ZnP^*$ (Fig. 17). Upon forming the supramolecular triad ($C_{60}$∼Im→ZnP∼BDP), the $^1ZnP^*$ moiety resulted in efficient electron transfer to the coordinated fullerene resulting in $C_{60}^{\bullet-}$∼Im→$ZnP^{\bullet+}$∼BDP ($k_{CS}^{singlet} = 4.7 \times 10^9\ s^{-1}$; $\Phi_{CS}^{singlet} = 0.9$) as revealed from Fig. 18. The absorption band of the $C_{60}^{\bullet-}$ moiety in $C_{60}^{\bullet-}$∼Im→$ZnP^{\bullet+}$∼BDP was detected by the nanosecond transient absorption spectra by the selective excitation of the BDP moiety (Fig. 19), confirming the charge-separation process followed by the energy-transfer process, as illustrated in Fig. 16. The observed electron transfer followed by energy transfer in the supramolecular triad mimicked the events of natural photosynthesis. That is, the BDP entity acts as antenna that absorbs light energy and transports spatially to the photosynthetic reaction center, while the electron transfer from the excited zinc porphyrin to fullerene mimicked the primary events of the reaction center where conversion of the electronic excitation energy to chemical

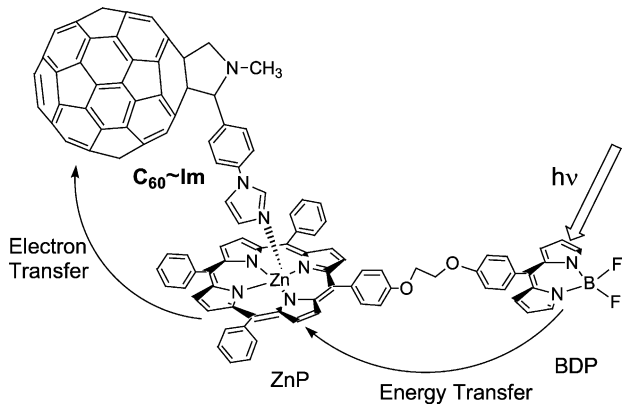


Fig. 16. Supramolecular boron dipyyrin (BDP), zinc porphyrin (ZnP) and fulleropyrrolidine ($C_{60}$∼Im) triad utilized to mimic the 'combined antenna-reaction center' events of photosynthesis.

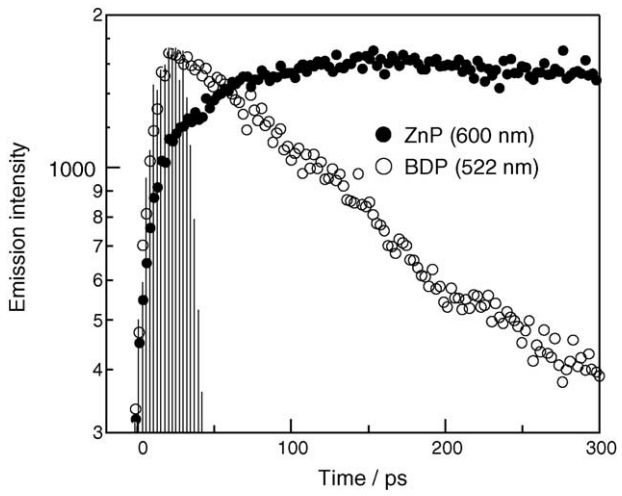


Fig. 17. Fluorescence rise time-profile at 600 nm for ZnP and decay time-profile at 522 nm for BDP of the ZnP-BDP dyad in *o*-DCB. The sample was excited at 388 nm and hatched area shows pulse profile.

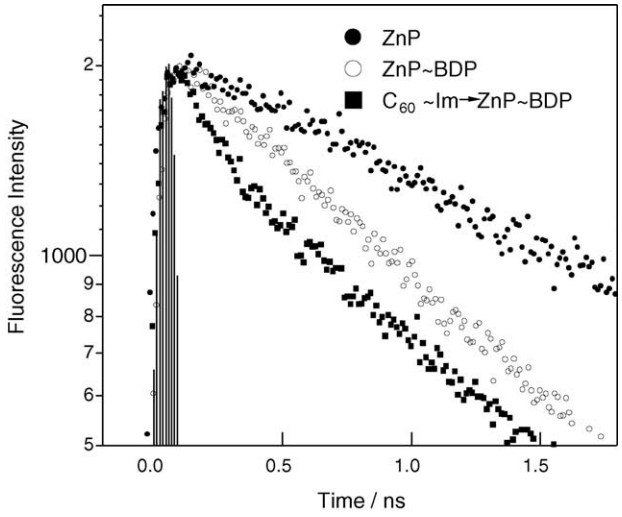


Fig. 18. Fluorescence decay time-profiles at 600 nm of ZnP, ZnP∼BDP, and supramolecular triad formed by coordinating $C_{60}$∼Im to ZnP∼BDP in *o*-DCB. The samples were excited at 550 nm.

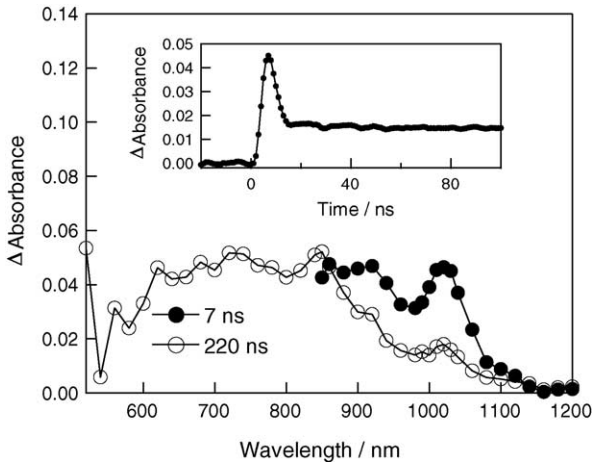


Fig. 19. Nanosecond transient absorption spectra of supramolecular triad formed by mixing $C_{60}$∼Im (0.25 mM) and ZnP∼BDP (0.05 mM) in *o*-DCB at 7 ns (●) and 160 ns (○) after the 500 nm laser irradiation. Inset: Absorption–time profiles at 1020 nm.

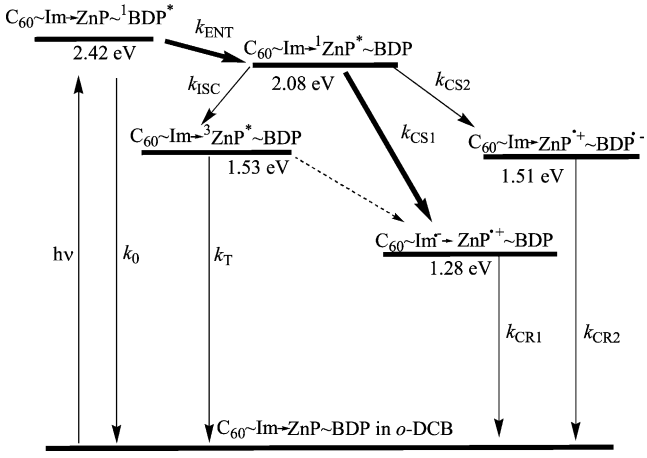


Fig. 20. Energy level diagram showing different photochemical events of supramolecular $C_{60}$∼Im→ZnP∼BDP triad after excitation of the BDP moiety.

energy in the form of charge separation would occurs. The important feature of the model system was in its relative 'simplicity' because of the utilized supramolecular approach to mimic rather complex 'combined antenna-reaction center' events of photosynthesis. The detail data are summarized in Table 2. The energy diagram is shown in Fig. 20, which reasonably interprets the all the observed processes.

Unique supramolecular triads were formed by a "covalent-coordinate" approach, where a free base porphyrin was functionalized to bear a $C_{60}$ appended with a pyridine group ($H_2P$∼$C_{60}$∼Py) capable of axial ligation with ZnTPP (Fig. 21) [78,80]. Steady-state fluorescence experiments were performed on the supramolecular triad system. Upon addition of $H_2P$∼$C_{60}$∼Py to a solution containing ZnTPP, the two emission bands of ZnTPP at 598 and 646 nm were quenched, accompanied by the appearance of two new emission bands at 665 and 720 nm, corresponding to the emission of $H_2$TPP. These data indicate that an energy-transfer process from $^1H_2P^*$ to ZnTPP is occurring within the self-assembled supramolecular triad system.

Picosecond time-resolved fluorescence spectral studies were performed on the covalently linked dyad systems. The short excited state lifetimes for the studied dyads (440–710 ps) indicate that an intramolecular charges separation process takes place from $^1H_2P^*$. The $k_{CS}$ value for the dyads were found to be $2.2 \times 10^9\ s^{-1}$. Time-resolved fluorescence spectra were also obtained for the self-assembled triad system with ZnTPP. For the triad systems, the fluorescence quenching of $^1$ZnTPP$^*$ was slightly accelerated on addition of $H_2P$∼$C_{60}$∼Py; the lifetimes of $^1$ZnTPP$^*$ of $H_2P$∼$C_{60}$∼Py→ZnTPP were found to be 1.78–1.83 ns, respectively, while the lifetime of uncoordinated ZnTPP was 2.10 ns. Nanosecond transient absorption spectral studies were performed to determine the nature of the processes via the excited state in the dyad and triad systems (Fig. 22). The relative efficiency of intermolecular electron transfer was

Table 2
Singlet energy-transfer rate-constants ($k_{ENT}^{singlet}$), energy-transfer efficiency ($\Phi_{ENT}^{singlet}$), charge-separation rate-constants ($k_{CS}^{singlet}$), and charge-separation quantum-yields ($\Phi_{CS}^{singlet}$) for dyad and supramolecular triad in *o*-DCB [90]

| Compound | $k_{ENT}^{singlet}$ ($s^{-1}$)[a] | $\Phi_{ENT}^{singlet}$[a] | $k_{CS}^{singlet}$ ($s^{-1}$)[b] | $\Phi_{CS}^{singlet}$[b] | $k_{CS}^{singlet}$ ($s^{-1}$)[c] | $\Phi_{CS}^{singlet}$[c] | $k_{CR}$ ($s^{-1}$)[d] |
|---|---|---|---|---|---|---|---|
| | (ZnP∼$^1$BDP$^*$)[a] | | ($^1$ZnP$^*$∼BDP)[b] | | (C$_{60}$∼Im→$^1$ZnP$^*$∼BDP)[c] | | |
| ZnP∼BDP | $9.2 \times 10^9$ | 0.83 | $3.1 \times 10^8$[e] | 0.38[e] | – | – | |
| $C_{60}$∼Im→ZnP∼BDP | $8.9 \times 10^9$ | 0.84 | $2.5 \times 10^8$[f] | (0.21)[f] | $4.7 \times 10^9$[g] | (0.34)[g] | $2.0 \times 10^8$ |

[a] Energy transfer from $^1$BDP$^*$ to ZnP. Calculated by following equations; $k_{ENT}^{singlet} = \tau_{F,ZnP\sim BDP^*}{}^{-1} - \tau_{F,BDP^*}{}^{-1}$ and $\Phi_{ENT}^{singlet} = (\tau_{F,ZnP\sim BDP^*}{}^{-1} - \tau_{F,BDP^*}{}^{-1})/\tau_{F,ZnP\sim BDP^*}{}^{-1}$.
[b] Charge separation between $^1$ZnP$^*$ and BDP.
[c] Charge separation between $^1$ZnP$^*$ and $C_{60}$Im.
[d] From the fast decay part at 1000 nm in the nanosecond transient absorption measurement.
[e] Calculated by following equations; $k_{CS}^{singlet} = \tau_{F,ZnP^*\sim BDP}{}^{-1} - \tau_{F,ZnP^*}{}^{-1}$ and $\Phi_{CS}^{singlet} = (\tau_{F,ZnP^*\sim BDP}{}^{-1} - \tau_{F,ZnP^*}{}^{-1})/\tau_{F,ZnP^*\sim BDP}{}^{-1}$.
[f] Calculated from slow decay part of ZnP$^*$ by following equations; $k_{CS}^{singlet} = \tau_{F,C60\sim Im\rightarrow ZnP^*\sim BDP}{}^{-1} - \tau_{F,ZnP^*}{}^{-1}$ and $\Phi_{CS}^{singlet} = (\tau_{F,C60\sim Im\rightarrow ZnP^*\sim BDP}{}^{-1} - \tau_{F,ZnP^*}{}^{-1})/\tau_{F,ZnP^*\sim BDP}{}^{-1}$ after multiplying the fraction.
[g] Calculated from fast decay part of $^1$ZnP$^*$ by equations above.

Table 3
Fluorescence lifetimes ($\tau_f$), charge-separation rate-constants ($k_{CS}$)[a], charge separation quantum-yields ($\Phi_{CS}$) of the covalently linked dyads and supramolecular triads in *o*-DCB and PhCN [78]

| Compound[b] | Solvent | $\lambda_{em}$ (nm) | $\tau_f$ (ns, %) | | $k_{CS}$ ($s^{-1}$) | $\Phi_{CS}$[c] |
|---|---|---|---|---|---|---|
| ZnTPP | *o*-DCB | 600 | 2.10 (100) | | – | – |
| $H_2P{\sim}C_{60}{\sim}Py$ | *o*-DCB | 720 | 0.44 (38) | 1.46 (62) | $2.2 \times 10^9$ | 0.97 |
| $H_2P{\sim}C_{60}{\sim}Py$[b] | PhCN | 720 | 0.43 (63) | 1.96 (37) | $2.2 \times 10^9$ | 0.97 |
| $H_2P{\sim}C_{60}{\sim}Py + ZnP$ (6:1)[d] | *o*-DCB | 600 | 1.78 (100) | | $8.5 \times 10^7$ | (0.03)[e] |
| | | 720 | 0.47 (40) | 1.49 (60) | $2.1 \times 10^9$ | 0.97 |
| $H_2P{\sim}C_{60}{\sim}Py + ZnP$ (1:1)[b] | *o*-DCB | 600 | 1.99 (100) | | $2.6 \times 10^7$ | (0.01)[e] |

[a] Short lifetime was employed for $\tau_f$ for bi-exponential decay. The $\tau_f$ value = 13.6 ns was employed for $H_2P$.
[b] For abbreviations, see Fig. 21.
[c] $\Phi_{CS}$ in parenthesis is calculated as ratio of the calculated $k_{CS}$.
[d] Concentration of porphyrin used = 0.04 mM; $\lambda_{ex}$ = 410 nm.
[e] The estimated $k_{CR}$ for the present dyads and triads is approximately $5.0 \times 10^7$ $s^{-1}$.

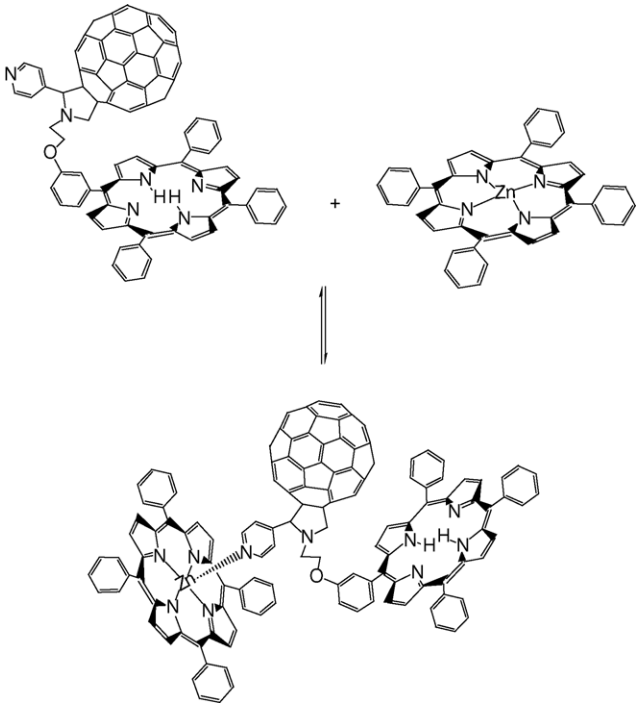

Fig. 21. Structure of free-base porphyrin–fullerene self-assembled to zinc porphyrin supramolecular triads.

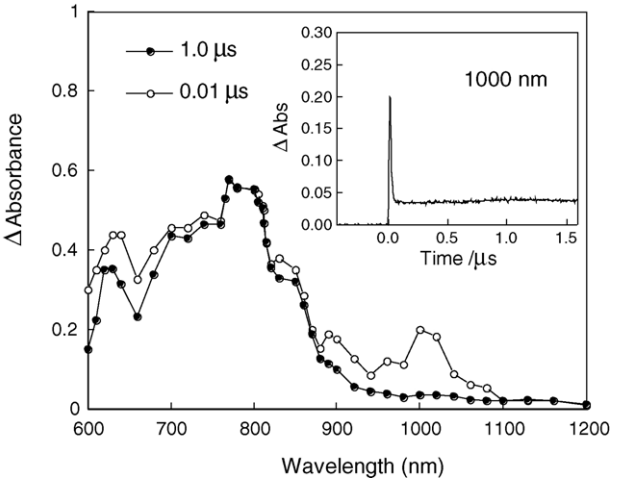


Fig. 22. Nanosecond transient absorption spectra obtained by the 532 nm laser photolysis of $H_2P{\sim}C_{60}{\sim}Py$ and ZnP (6:1) in *o*-DCB; (◯) 0.01 μs and (●) 1 μs. Inset: time-profile at 1000 nm.

evaluated by monitoring the absorbance ratio of the transient absorption bands at 700 and 1000 nm ($A_{1000\,nm}/A_{700\,nm}$). For $H_2P{\sim}C_{60}{\sim}Py$, this ratio was determined to be 0.45. Under the conditions of 6:1 of $[H_2P{\sim}C_{60}{\sim}Py]$:[ZnTPP] where almost all ZnTPP is coordinated, the absorbance ratio ($A_{1000\,nm}/A_{700\,nm}$) increased to 0.50. These data indicate that the efficiency of the charges-separated state ($H_2P{\sim}C_{60}^{\bullet-}{\sim}Py{\rightarrow}ZnTPP^{\bullet+}$) increases upon complex formation. Table 3 lists all of the photochemical kinetic data.

## 3. Concluding remarks

The porphyrins, phthalocyanines and fullerenes have been found to be excellent building blocks for supramolecular systems for the study of photoinduced energy and electron transfer reactions by using time-resolved ultrafast spectroscopic techniques. In the supramolecular conjugates formed by axial coordination, the charge separation process occurs mainly from the singlet excited states of the porphyrins and phthalocyanines acting as electron donor. In some of the reported donor–acceptor conjugates, the predicted acceleration of the charge separation process and deceleration of the charge recombination process have been observed. The photochemical properties of the porphyrin/phthalocyanine and fullerene moieties were shown to be tuned in a controlled manner upon coordination to metal center. The nature of the linker between the donor and acceptor entities, the solvent, and the metal ions in the porphyrin/phthalocyanine cavity is shown to affect the overall self-assembly process and photochemical reactivity. Studies on self-assembled supramolecular triads, tetrads, etc., are only in the beginning stages, and future studies will be anticipated to involve more complex systems targeted for better charge stabilization, and also to perform specific light-driven photochemical processes, such as the one shown for 'energy transfer followed by electron transfer' in the supramolecular triad.

As a final note, from the synthetic point although the supramolecular strategy is more convenient compared with the covalent bonding strategy, more polar solvents destroy the supramolecular systems, hence, long-lived charge-separation states are difficult to establish. Further efforts with respect to better design of the porphyrin/phthalocyanines–fullerene conjugates are needed to improve the lifetimes of the charge-separated state. The supramolecular approach of building fullerene–porphyrin and fullerene–phthalocyanine conjugates is beginning to provide well-characterized donor–acceptor systems, which could eventually be used for the development of solar energy harvesting and opto-electronic devices such as sensors, switches, gates, etc.

## Acknowledgments

The authors are thankful to the donors of the Petroleum Research Fund (administered by the American Chemical Society), the National Institutes of Health (to FD), the Japan Ministry of Education, Science, Technology, Culture and Sports (to OI, Priority Area 417), for support of this research.

## References

[1] J. Deisenhofer, J.R. Norris (Eds.), The Photosynthetic Reaction Center, Academic Press, San Diego, 1993.
[2] R.E. Blankenship, M.T. Madigan, C.E. Bauer (Eds.), Anoxygenic Photosynthetic Bacteria, Kluwer Academic Publishers, Dordrecht, 1995.
[3] C. Kirmaier, D. Holton, in: J. Deisenhofer, J.R. Norris (Eds.), The Photosynthetic Reaction Center, vol. II, Academic Press, San Diego, 1993, p. 49.
[4] R.A. Marcus, Angew. Chem. Int. Ed. Engl. 32 (1993) 1111.
[5] M. Bixon, J. Jortner, Adv. Chem. Phys. 106 (1999) 35.
[6] M.D. Newton, Chem. Rev. 91 (1991) 767.
[7] H.D. Roth, A brief history of photoinduced electron transfer and related reactions, in: J. Mattay (Ed.), Topics in Current Chemistry, vol. 156, Springe-Verlage, Berlin, 1990, p. 1.
[8] J.S. Connolly, J.R. Bolton, in: M.A. Fox, M. Chanon (Eds.), Photoinduced Electron Transfer, Elsevier, Amsterdam, 1988.
[9] G.J. Kavarnos, N.G. Turro, Chem. Rev. 86 (1986) 401.
[10] S. Mattes, S. Farid, Science 226 (1984) 917.
[11] D.F. Eaton, Electron transfer process in imaging, in: J. Mattay (Ed.), Topics in Current Chemistry, Springe-Verlage, Berlin, 1990, p. 199.
[12] M.R. Wasielewski, Chem. Rev. 92 (1992) 435.
[13] G.J. Kavarnos (Ed.), Fundamentals of Photoinduced Electron Transfer, VCH Publisher, New York, 1993, p. 103.
[14] J.S. Connolly (Ed.), Photochemical Conversion and Storage of Solar Energy, Academic, New York, 1981.
[15] V. Balzani (Ed.), Electron Transfer in Chemistry, vols. I–V, Wiley-VCH, Weinheim, 2001.
[16] G. McLendon, R. Hake, Chem. Rev. 92 (1992) 481.
[17] I.R. Gould, S. Farid, Acc. Chem. Res. 29 (1996) 522.
[18] N. Mataga, H. Miyasaka, Adv. Chem. Phys. 107 (1999) 431.
[19] F.D. Lewis, R.L. Letsinger, M.R. Wasielewski, Acc. Chem. Res. 34 (2001) 159.
[20] H. Kurreck, M. Huber, Angew. Chem., Int. Ed. Engl. 34 (1995) 849.
[21] M.-J. Blanco, M.C. Jiménez, J.-C. Chambron, V. Heitz, M. Linke, J.-P. Sauvage, Chem. Soc. Rev. 28 (1999) 293.
[22] V. Balzani, A. Juris, M. Venturi, S. Campagna, S. Serroni, Chem. Rev. 96 (1996) 759.
[23] M.N. Paddon-Row, Acc. Chem. Res. 27 (1994) 18.
[24] J.W. Verhoeven, Adv. Chem. Phys. 106 (1999) 603.
[25] A. Osuka, N. Mataga, T. Okada, Pure Appl. Chem. 69 (1997) 797.
[26] L. Sun, L. Hammarström, B. Åkermark, S. Styring, Chem. Soc. Rev. 30 (2001) 36.
[27] K. Yoshihara, S. Kumazaki, J. Photochem. Photobiol. C: Rev. 1 (2000) 22.
[28] S. Takagi, H. Inoue, in: V. Ramamurthy, K.S. Schanze (Eds.), Multimetallic and Macromolecular Inorganic Photochemistry, Marcel Dekker, New York, 1999, p. 215.
[29] P. Piotrowiak, Chem. Soc. Rev. 28 (1999) 143.
[30] H. Imahori, Y. Sakata, Adv. Mater. 9 (1997) 537.
[31] D.M. Guldi, M. Prato, Acc. Chem. Res. 33 (2000) 695.
[32] D. Gust, T.A. Moore, in: K.M. Kadish, K. Smith, R. Guilard (Eds.), The Porphyrin Handbook, vol. 8, Academic Press, San Diego, 2000, p. 153.
[33] J.S. Sessler, B. Wang, S.L. Springs, C.T. Brown, in: J.L. Atwood, J.E.D. Davies, D.D. MacNicol, F. Vögtle (Eds.), Comprehensive Supramolecular Chemistry, Pergamon, 1996 (Chapter 9).
[34] T. Hayashi, H. Ogoshi, Chem. Soc. Rev. 26 (1997) 355.
[35] M.W. Ward, Chem. Soc. Rev. 26 (1997) 365.
[36] M.E. El-Khouly, O. Ito, P.M. Smith, F. D'Souza, J. Photochem. Photobiol. C: Rev. 5 (2004) 79.
[37] M.C. Petty, M.R. Bryce, D. Bloor (Eds.), Introduction of Molecular Electronics, Oxford University Press, New York, 1995.
[38] B.L. Feringa (Ed.), Molecular Switches, Wiley-VCH GmbH, Weinheim, 2001.
[39] A. Hirsch (Ed.), Fullerene and Related Structures, vol. 199, Springer, Berlin, 1999.
[40] C.S. Foote, in: K. Prassides (Ed.), Physics and Chemistry of the Fullerenes, Kluwer Academic Publishers, Amsterdam, 1994, p. 79.
[41] D.M. Guldi, P.V. Kamat, in: K.M. Kadish, R.S. Ruoff (Eds.), Fullerenes, Chemistry, Physics and Technology, Wiley-Interscience, New York, 2000, p. 225.
[42] H. Imahori, K. Hagiwara, T. Akiyama, M. Akoi, S. Taniguchi, T. Okada, M. Shirakawa, Y. Sakata, Chem. Phys. Lett. 263 (1996) 545.
[43] D.M. Guldi, K.-D. Asmus, J. Am. Chem. Soc. 119 (1997) 5744.
[44] H. Imahori, M.E. El-Khouly, M. Fujitsuka, O. Ito, Y. Sakata, S. Fukuzumi, J. Phys. Chem. A 105 (2001) 325.
[45] S. Nath, H. Pal, A.V. Sapre, Chem. Phys. Lett. 360 (2002) 422.
[46] F. Diederich, C. Thilgen, Science 271 (1996) 317.
[47] A. Hirsch (Ed.), The Chemistry of the Fullerenes, Georg Thieme, Stuttgart, 1994.
[48] Q. Xie, E. Perez-Cordero, L. Echegoyen, J. Am. Chem. Soc. 114 (1992) 3978.
[49] J.-F. Nierengarten, J.-F. Eckert, D. Felder, J.-F. Nicoud, N. Armaroli, G. Marconi, V. Vicinelli, C. Boudon, J.-P. Gisselbrecht, M. Gross, G. Hadziioannou, V. Krasilkov, L. Ouali, L. Echegoyen, S.-G. Liu, Carbon 38 (2000) 1587.
[50] P.M. Allemand, A. Koch, F. Wudl, Y. Rubin, F. Diederich, M.M. Alvarez, S.J. Anz, R.L. Whetten, J. Am. Chem. Soc. 113 (1991) 1050.
[51] D. Dubois, K.M. Kadish, S. Flanagan, R.E. Haufler, L.P.F. Chibante, L.J. Wilson, J. Am. Chem. Soc. 114 (1992) 4364.
[52] M.M. Alam, A. Watanabe, O. Ito, Bull. Chem. Soc. Jpn. 70 (1997) 1833.
[53] A. Watanabe, O. Ito, J. Phys. Chem. 98 (1994) 7736.
[54] O. Ito, Y. Sasaki, Y. Yoshikawa, A. Watanabe, J. Phys. Chem. 99 (1995) 9838.
[55] T. Nojiri, A. Watanabe, O. Ito, J. Phys. Chem. A 102 (1998) 5215.
[56] M.E. El-Khouly, Y. Araki, M. Fujitsuka, O. Ito, Phys. Chem. Chem. Phys. 4 (2002) 3322.
[57] M.E. El-Khouly, L.M. Rogers, M.E. Zandler, S. Gadde, M. Fujitsuka, O. Ito, F. D'Souza, Chem. Phys. Chem. 4 (2003) 474.

[58] T. Nojiri, M.M. Alam, H. Konami, A. Watanabe, O. Ito, J. Phys. Chem. A 101 (1997) 7943.
[59] P.A. Liddell, D. Kuciauskas, J.P. Sumida, B. Nash, D. Nguyen, A.L. Moore, T.A. Moore, D. Gust, J. Am. Chem. Soc. 119 (1997) 1400.
[60] H. Imahori, K. Tamaki, D.M. Guldi, C. Luo, M. Fujitsuka, O. Ito, Y. Sakata, S. Fukuzumi, J. Am. Chem. Soc. 123 (2001) 2607.
[61] H. Imahori, Y. Sekiguchi, Y. Kashiwagi, T. Sato, Y. Araki, O. Ito, H. Yamada, S. Fukuzumi, Chem. Eur. J. 11 (2004) 3184.
[62] H. Imahori, K. Tamaki, Y. Araki, Y. Sekiguchi, O. Ito, Y. Sakata, S. Fukuzumi, J. Am. Chem. Soc. 124 (2002) 5165.
[63] P.A. Liddell, G. Kodis, A.L. Moore, T.A. Moore, D. Gust, J. Am. Chem. Soc. 124 (2002) 7668.
[64] K. Li, D.I. Schuster, D.M. Guldi, M.A. Herranz, L. Echegoyen, J. Am. Chem. Soc. 126 (2004) 3388.
[65] S.N. Smirnov, P.A. Liddell, I.V. Vlassiouk, A. Teslja, D. Kuciauskas, C.L. Braun, A.L. Moore, T.A. Moore, D. Gust, J. Phys. Chem. A 107 (2003) 7567.
[66] H. Imahori, Y. Mori, J. Matano, J. Photochem. Photobiol C: Photochem. Rev. 4 (2003) 51.
[67] A.L. Balch, M.M. Olmstead, Chem. Rev. 98 (1998) 2123.
[68] J.D. Crane, P.B. Hitchcock, H.W. Kroto, R. Taylor, D.R.M. Walton, J. Chem. Soc., Chem. Commun. (1992) 1764.
[69] K.M. Kadish, K.M. Smith, R. Guilard (Eds.), The Porphyrin Handbook, vols. 1–10, Academic Press, Burlington, MA, 2000.
[70] M. Gouterman, in: D. Dolphin (Ed.), Porphyrins, vol. III, Academic Press, New York, 1978.
[71] A.J. Hoff, J. Amesz, in: H. Scheer (Ed.), Chlorophylls, CRC Press, Boca Raton, 1992, p. 723.
[72] M.E. El-Khouly, S.D.-M. Islam, M. Fujitsuka, O. Ito, J. Porphyrins Phthalocyanines 4 (2000) 713.
[73] C.C. Lenzoff, A.Z.P. Lever (Eds.), Phthalocyanines, Properties and Applications, VCH Publishers Inc., New York, 1989.
[74] T. Da Ros, M. Prato, D.M. Guldi, M. Ruzzi, L. Pasimeni, Chem. Eur. J. 7 (2001) 816.
[75] D.M. Guldi, C. Luo, T. Da Ros, M. Prato, E. Dietel, A. Hirsch, Chem. Commun. (2000) 375.
[76] D.M. Guldi, C. Luo, A. Swartz, M. Scheloske, A. Hirsch, Chem. Commun. (2001) 1066.
[77] F. Diederich, M.G. Lopez, Chem. Soc. Rev. 28 (1999) 263.
[78] F. D'Souza, G.D. Deviprasad, M.E. El-Khouly, M. Fujitsuka, O. Ito, J. Am. Chem. Soc. 123 (2001) 5277.
[79] F. D'Souza, G.R. Deviprasad, M.E. Zandler, V.T. Hoang, K. Arkady, M. van Stipdonk, A. Perera, M.E. El-Khouly, M. Fujitsuka, O. Ito, J. Phys. Chem. A 106 (2002) 3243.
[80] F. D'Souza, G.R. Deviprasad, M.E. Zandler, M.E. El-Khouly, M. Fujitsuka, O. Ito, J. Phys. Chem. B 106 (2002) 4952.
[81] G. Yin, D. Xu, Z. Xu, Chem. Phys. Lett. 365 (2002) 232.
[82] F. D'Souza, G.R. Deviprasad, M.S. Rahman, J.-P. Choi, Inorg. Chem. 38 (1999) 2157.
[83] N. Armaroli, F. Diederich, L. Echegoyen, T. Habicher, L. Flamigni, G. Marconi, J.-F. Nierengarten, New J. Chem. 21 (1999) 77.
[84] T. Da Ros, M. Prato, D.M. Guldi, E. Alessio, M. Ruzzi, L. Pasimeni, Chem. Commun. (1999) 635.
[85] F. D'Souza, N.P. Rath, G.R. Deviprasad, M.E. Zandler, Chem. Commun. (2001) 267.
[86] S.R. Wilson, S. MacMahon, F.T. Tat, P.D. Jarowski, D.I. Schuster, Chem. Commun. (2003) 226.
[87] F. D'Souza, G.R. Deviprasad, M.E. Zandler, M.E. El-Khouly, M. Fujitsuka, O. Ito, J. Phys. Chem. A 107 (2003) 4801.
[88] F. D'Souza, S. Gadde, M.E. Zandler, K. Arkady, M.E. El-Khouly, M. Fujitsuka, O. Ito, J. Phys. Chem. A 106 (2002) 12393.
[89] F. D'Souza, P.M. Smith, S. Gadde, A.L. McCarty, M.J. Kullman, M.E. Zandler, M. Itou, Y. Araki, O. Ito, J. Phys. Chem. B 108 (2004) 11333.
[90] F. D'Souza, P.M. Smith, M.E. Zandler, A.L. McCarty, M. Itou, Y. Araki, O. Ito, J. Am. Chem. Soc. 126 (2004) 7898.